Stereochemical Analysis of Palladium(II) Complexes of the Selenium Coronands 1,5,9,13-Tetraselenacyclohexadecane and 1,5,9,13,17,21-Hexaselenacyclotetracosane

Raymond J. Batchelor, Frederick W. B. Einstein, Ian D. Gay, Jian Gu, B. Mario Pinto,* and Xuemin Zhou

Department of Chemistry, Simon Fraser University, Burnaby, B.C. V5A 1S6, Canada

Received August 29, 1995[⊗]

Crystal structures for $[Pd(16Se4)][BF_4]_2$ (**1**) (16Se4 = 1,5,9,13-tetraselenacyclohexadecane) and $[Pd(16Se4)][BF_4]Cl$ (**2**) both contain the $[Pd(16Se4)]^{2+}$ ion which has square-planar coordination about Pd and a stereochemistry (denoted *c,c,c*) in which all of the selenium nonbonding valence electron pairs are mutually *cis* with respect to the coordination plane. In both structures the conformation adopted by the cation deviates slightly but significantly from molecular *mm* (C_{2v}) symmetry. The asymmetry is most clearly resolved for **2**, in which the Pd−Se bond lengths vary significantly (2.444(1)−2.463(1) Å). For **1**: $T = 295$ K; fw = 764.2; space group *Pnma*; $Z = 4$; $a = 12.356(1)$ Å; $b = 10.397(1)$ Å; $c = 16.233(2)$ Å; $V = 2193.7$ Å^3; $R_F = 0.036$ for 997 data ($I_o \geq 2.5\sigma(I_o)$) and 131 variables. For **2**: $T = 295$ K; fw = 712.8; space group $P\bar{1}$; $Z = 2$; $a = 7.2377(4)$ Å; $b = 10.7784(7)$ Å; $c = 12.9523(9)$ Å; $\alpha = 76.607(6)°$; $\beta = 86.020(6)°$; $\gamma = 85.186(5)°$; $V = 978.17$ Å^3; $R_F = 0.023$ for 2134 data ($I_o \geq 2.5\sigma(I_o)$) and 214 variables. The ^{77}Se, ^{1}H, ^{13}C, and ^{1}H−^{13}C correlated NMR spectra for **1** in D_2O solution were fully assigned. At room temperature, $[Pd(16Se4)]^{2+}$ occurs in D_2O solution predominantly as the *c,t,c* and *c,c,c* stereoisomers. Variable temperature NMR spectroscopic results demonstrate that at an elevated temperature (389 K) configurational interconversion is rapid on the ^{1}H-NMR time scale. Cyclic voltammetry of **1** and **2**, in MeCN solution with Pt electrodes, shows that the redox reaction of the pair Pd(II)/Pd(I) is irreversible with cathodic peak potentials at −0.56 and −0.47 V vs SCE, respectively. The crystal structure of $[(PdCl)_2(24Se6)][BF_4]_2 \cdot 2CH_2Cl_2$ (**3**$\cdot 2CH_2Cl_2$) reveals a complex dication in which two individual palladium(II) centers are each bound by three adjacent selenium atoms. Both palladium centers display square planar coordination with a chlorine atom occupying the fourth site. The complex exhibits trans relationships between adjacent pyramidal selenium centers and adopts a conformation which has only approximate *m* (C_s) symmetry. The mutually *trans* Pd−Se bond lengths range from 2.421(1) to 2.428(1) Å. The Pd−Se bond lengths *trans* to the chlorine atom are 2.372(1) and 2.364(1) Å, and the corresponding Pd−Cl bond lengths are 2.343(2) and 2.351(3) Å. For **3**$\cdot 2CH_2Cl_2$: $T = 195$ K; monoclinic, space group $P2_1/c$; $Z = 4$; $a = 16.421(2)$ Å; $b = 19.353(2)$ Å; $c = 12.397(3)$ Å; $\beta = 91.16(2)°$; $V = 3938.9$ Å^2; $R_F = 0.037$ for 3793 data ($I_o \geq 2.5\sigma(I_o)$) and 409 variables. Cyclic voltammetry of **3** in MeCN solution with Pt electrodes shows an irreversible cathodic peak potential at −0.58 V vs SCE corresponding to a Pd(II)/Pd(I) pair. Electrolysis in MeCN confirms that this is a two-electron reduction for the complex.

Introduction

The coordination chemistry of thia macrocycles has attracted intense interest.[1] However, reports on the metal-ion complexes of the selenium congeners are relatively scarce and have dealt mainly with the ligand 1,5,9,13-tetraselenacyclohexadecane (16Se4).[2] To date, we have reported the electron transfer reaction of the metal-ion complex of a selenium coronand, a Cu(II) complex of 16Se4.[3] Recently, reports of complexes of 16Se4, with Rh(III),[4] Pd(II), and Pt(II)[5] have also appeared. We have also reported the study of the adducts of 16Se4 with copper(I) triflate and mercury(II) cyanide[6] and communicated our results on Cu(I), Cu(II), and Pd(II) complexes of 16Se4 and other selenium coronands.[7] Reports of transition metal-ion complexation by monoselena[8] and diselena[9] macrocyclic ligands have also appeared.

Although a recent publication[5] reported the preparation of the complexes $[M(16Se4)][PF_6]_2 \cdot 2MeCN$ (M = Pd or Pt) and their variable temperature NMR spectra, little interpretation of these spectra in terms of the dynamic process under observation or the identity of stereoisomers was possible. We report here examples of Pd(II) complexes with 16Se4 ($[Pd(16Se4)][BF_4]_2$ (**1**) and $[Pd(16Se4)][BF_4]Cl$ (**2**)) that possess the *c,c,c* configuration (*cis*, *cis*, *cis* for the orientations, with respect to the coordination plane of the coronand, of successive pyramidal donor atom environments[10]). In all cases of metal-ion complexation to 16Se4 reported to date, the stereochemistry of ligation in the solid state was *c,t,c*. We report also the stereodynamics of **1** in solution and its electrochemical characterization. The crystal and molecular structure of a complex

[⊗] Abstract published in *Advance ACS Abstracts,* May 1, 1996.

(1) For example: Cooper, S. R.; Rawle, S. C. *Struct. Bonding (Berlin)* **1990**, *72*, 1. Blake, A. J.; Schröder, M. In *Advances in Inorganic Chemistry*; Sykes, A. G., Ed.; Academic: New York, 1990; Vol. 35, pp 2−80.
(2) Batchelor, R. J.; Einstein, F. W. B.; Gay, I. D.; Gu, J. H.; Johnston, B. D.; Pinto, B. M. *J. Am Chem. Soc.* **1989**, *111*, 6582.
(3) Batchelor, R. J.; Einstein, F. W. B.; Gay, I. D.; Gu, J. H.; Pinto, B. M.; Zhou, X.-M. *J. Am. Chem. Soc.* **1990**, *112*, 3706.
(4) Kelly, P. F.; Levason, W.; Reid, G.; Williams, D. J. *J. Chem. Soc., Chem. Commun.* **1993**, 1716.
(5) Champness, N. R.; Kelly, P. F.; Levason, W.; Reid, G.; Slawin, A. M. Z.; Williams, D. J. *Inorg. Chem.* **1995**, *34*, 651.
(6) Batchelor, R. J.; Einstein, F. W. B.; Gay, I. D.; Gu, J.-H.; Pinto, B. M. *J. Organomet. Chem.* **1991**, *411*, 147.
(7) Pinto, B. M., Batchelor, R. J.; Einstein, F. W. B.; Gay, I. D.; Gu, J.; Zhou, X. *76th Canadian Society for Chemistry Conference*, Sherbrooke, Quebec, June, 1993; Canadian Society for Chemistry: Sherbrooke, Canada, 1993; Abstract 683.
(8) Xu, H.; Li, W.; Liu, X. *Youji Huaxue* **1993**, *13*, 52.
(9) Kumagai, T.; Akabori, S. *Chem. Lett.* **1989**, 1667.
(10) Ferguson, G.; McCrindle, R.; McAlees, A. J.; Parvez, M.; Stephenson, D. K. *J. Chem. Soc., Dalton Trans.* **1983**, 1865.

S0020-1669(95)01151-7 CCC: $12.00

of 1,5,9,13,17,21-hexaselenacyclotetracosane (24Se6)[2] with Pd(II) ($[(PdCl)_2(24Se6)][BF_4]_2 \cdot 2CH_2Cl_2$ (**3**·$2CH_2Cl_2$)) is also described.

Experimental Section

General Information. NMR spectra were recorded on a Bruker AMX-400 NMR spectrometer operating at 400.13, 100.6, and 76.3 MHz for ^{1}H, ^{13}C, and ^{77}Se, respectively. For the ^{1}H-NMR and ^{13}C-NMR spectra, chemical shifts are with respect to $SiMe_4$; coupling constants were obtained from a first-order analysis of the spectra. For the ^{77}Se spectra chemical shifts are reported with respect to external Me_2Se. The ^{1}H-homonuclear chemical-shift correlated (COSY) spectra were acquired with initial data sets of 512 × 2048 data points which were zero-filled once in the F_1 dimension to give a final data set of 1024 × 2048 real data points. For the inverse detection experiments, a four-pulse sequence was used for the ^{1}H{^{13}C}-^{13}C correlation;[11] the same sequence, incorporating a BIRD pulse in the preparation period, was used for the ^{1}H−^{13}C correlation.[12] In both cases, time proportional phase increments were used in F_1. The data sets of 512 × 1024 data points were zero-filled once in both the F_1- and the F_2-dimensions, to give a final data set of 1024 × 2048 real data points, with a digital resolution of 10.3 and 1.0 Hz/pt in the F_1- and F_2-dimensions, respectively.

UV−visible spectra were measured on a Hewlett-Packard HP 89500 UV/VIS Chem Station. The electron impact mass spectrum of **3**·$2CH_2Cl_2$ was measured on a Hewlett-Packard HP-5985 mass spectrometer with 70 eV ionizing voltage.

Cyclic voltammograms of N_2-purged acetonitrile solutions were recorded on a PAR Model 173/175 electrochemistry system. The reference electrode was an aqueous saturated calomel electrode (SCE) with a Luggin capillary. The working electrode was either a platinum plane or a carbon electrode and the counter electrode was a platinum wire. Electrolysis, in N_2-purged MeCN, was carried out in a two-compartment electrochemical cell with a sintered-glass partition. The working and counter electrodes were Pt gauze, and the reference electrode was aqueous saturated calomel with a Luggin capillary. Tetraethylammonium perchlorate (TEAP, 0.1 M) was used as the electrolyte.

Solvents were distilled before use and were dried, as necessary, by literature procedures. Melting points were determined on a Fisher-Johns melting point apparatus and are uncorrected. Microanalyses were performed by M. K. Yang of the Simon Fraser University Microanalytical Laboratory.

Synthesis. $[Pd(16Se4)](BF_4)_2$ (1). $PdCl_2$ (8.7 mg, 0.049 mmol) in MeCN (2 mL) under N_2 was warmed to effect dissolution, and $NaBF_4$ (13 mg, 0.12 mmol) was added to the yellow solution. The mixture was stirred for 10 min and cooled to ambient temperature. 16Se4 (23.8 mg, 0.049 mmol) was added, and the mixture was stirred for 30 min at ambient temperature and then filtered. Ether vapor diffusion into the yellow filtrate gave yellow crystals (21 mg, 57%). UV (MeCN, λ, nm (ϵ, M^{-1} cm^{-1})): 314 (26 758), 210 (8409) nm. ^{1}H NMR (CD_3CN): δ 2.30−2.75 (complex multiplets, rel integrated int 1); 3.04−3.53 (complex multiplets, rel integrated int 2). ^{13}C{^{1}H} NMR (D_2O): δ 26.3, 29.8, 30.0, (30.2 w), 33.6, 33.7, (34.2 w), 35.1. ^{77}Se NMR (D_2O): δ 152 (rel integrated int 1.6), 198 (rel integrated int 1). Anal. Calcd for $PdC_{12}H_{24}Se_4B_2F_8$: C, 18.86; H, 3.16. Found: C, 19.10; H, 3.11.

$[Pd(16Se4)Cl]BF_4$ (2). $PdCl_2$ (16.4 mg, 0.092 mmol) in MeCN/CH_2Cl_2 (4 mL, 2:1, v/v) under N_2 was warmed to effect dissolution, and $NaBF_4$ (20.3 mg, 0.18 mmol) was added to the yellow solution. The mixture was stirred for 5 min. 16Se4 (44.8 mg, 0.092 mmol) was added, and the mixture was stirred for 15 min at ambient temperature and then filtered. Ether vapor diffusion into the red filtrate gave red crystals (35 mg, 54%). UV (MeCN, λ, nm (ϵ, M^{-1} cm^{-1})): 314 (19 949), 210 (6548) nm. ^{1}H NMR (CD_3CN): δ 2.29−2.76 (complex multiplets, rel integrated int 1); 3.03−3.55 (complex multiplets, rel integrated int 2). Anal. Calcd for $PdC_{12}H_{24}Se_4ClBF_4$: C, 20.22; H, 3.39. Found: C, 20.28; H, 3.28.

Table 1. Crystallographic Data for the Structure Determinations of $[Pd(16Se4)][BF_4]_2$ (**1**), $[Pd(16Se4)][BF_4]Cl$ (**2**), and $[(PdCl)_2(24Se6)][BF_4]_2 \cdot 2CH_2Cl_2$ (**3**·$2CH_2Cl_2$)

	1	**2**	**3**·$2CH_2Cl_2$
formula	$PdSe_4F_8C_{12}B_2H_{24}$	$PdSe_4ClF_4C_{12}BH_{24}$	$Pd_2Se_6Cl_6F_8C_{20}B_2H_{40}$
cryst syst	orthorhombic	triclinic	monoclinic
fw	764.2	712.8	1353.42
space group	*Pnma*	$P\bar{1}$	$P2_1/c$
a[a] (Å)	12.356(1)	7.2377(4)	16.421(2)
b (Å)	10.937(1)	10.7784(7)	19.353(2)
c (Å)	16.233(2)	12.9523(9)	12.397(3)
α (deg)		76.607(6)	
β (deg)		86.020(6)	91.16(2)
γ (deg)		85.186(5)	
T (K)	295	295	195
V (Å^3)	2193.7	978.17	3938.9
Z	4	2	4
ρ_c (g cm^{-3})	2.314	2.420	2.282
λ(Mo Kα$_1$) (Å)	0.709 30	0.709 30	0.709 30
μ(Mo Kα) (cm^{-1})	74.69	84.74	68.6
cryst d (mm)	0.11 × 0.22 × 0.26	0.07 × 0.20 × 0.21	0.19 × 0.22 × 0.25
transmn[b]	0.211−0.486	0.218−0.575	0.275−0.385
2θ range (deg)	4−48	4−47	2−46
R_F[c]	0.036	0.022	0.037
R_{wF}[d]	0.047	0.027	0.047

[a] The unit cells were determined from 25 (**1** and **2**) and 23 (**3**·$2CH_2Cl_2$) well-centered reflections (**1** and **3**·$2CH_2Cl_2$, 30° ≤ 2θ ≤ 42°; **2,** 32° ≤ 2θ ≤ 42°). [b] The data were corrected for absorption by the Gaussian integration method. [c] $R_F = \Sigma||F_o| - |F_c||/\Sigma|F_o|$, for 997 (**1**), 2134 (**2**), and 3793 (**3**·$2CH_2Cl_2$) data ($I_o \geq 2.5\sigma(I_o)$). [d] $R_{wF} = [\Sigma(w(|F_o| - |F_c|)^2)/\Sigma(wF_o2)]^{1/2}$ for observed data (see *a*, above); $w = [\sigma(F_o)^2 + kF_o^2]^{-1}$, where k = 0.0005 (**1**), 0.0001 (**2**), and 0.0004 (**3**·$2CH_2Cl_2$).

$[(PdCl)_2(24Se6)][BF_4]_2$ (3). $PdCl_2$ (12.7 mg, 0.071 mmol) in MeCN (3 mL) under N_2 was heated to effect dissolution and then cooled to ambient temperature. 24Se6 (26.0 mg, 0.035 mmol) was added, and the mixture was stirred for 5 min. $NaBF_4$ (23 mg, 0.21 mmol) was then added. The mixture was stirred for 15 min and then filtered. Ether vapor diffusion into the yellow filtrate gave yellowish orange crystals (34.8 mg, 82%). UV (MeCN, λ, nm (ϵ, M^{-1} cm^{-1})): 366 (4837), 294 (24 838), 216 (13 145) nm. Anal. Calcd for $Pd_2C_{18}H_{36}Se_6Cl_2B_2F_8$: C, 18.26; H, 3.06. Found: C, 18.12; H, 3.00.

X-ray Crystallography. Complex scattering factors for neutral atoms[13] were used in the calculation of structure factors. The programs used for data reduction, structure solution, and graphical output were from the NRCVAX Crystal Structure System.[14] The program suite CRYSTALS[15] was employed in the refinement. Crystal and refinement data for the structures are shown in Table 1. A detailed description of the crystal structure determinations is included in the Supporting Information.

Results and Discussion

Pd(II) Complexes of 16Se4. $[Pd(16Se4)][BF_4]_2$ (**1**) was prepared by the method described and was obtained as yellow crystals. When the mixing time was shorter, the anion exchange was not complete, owing to the insolubility of $NaBF_4$, and $[Pd(16Se4)]ClBF_4$ (**2**) was isolated as red crystals. UV−visible absorption spectra of yellow MeCN solutions of **1** and **2** were

(11) Bax, A.; Griffey, R. H.; Hawkins, B. L. *J. Magn. Reson.* **1983**, *55*, 301.

(12) Bax, A.; Subramanian, S. *J. Magn. Reson.* **1986**, *67*, 565.

(13) *International Tables for X-ray Crystallography*; Kynoch: Birmingham, England, 1975; Vol. IV, p 99.

(14) Gabe, E. J.; LePage, Y.; Charland, J.-P.; Lee, F. L.; White, P. S. NRCVAX-An Interactive Program System for Structure Analysis. *J. Appl. Crystallogr.* **1989**, *22*, 384.

(15) Watkin, D. J.; Carruthers, J. R.; Betteridge, P. W. *CRYSTALS*; Chemical Crystallography Laboratory, University of Oxford: Oxford, England, 1984.

similar (λ_{max}, nm (ϵ, M^{-1} cm^{-1})): **1**, 314 (26 758), 210 (8409); **2**, 314 (19 949), 210 (6548).

Cyclic Voltammetry. The cyclic voltammogram of **1**, recorded with a platinum electrode in MeCN (0.1 M Et_4NClO_4), showed that the electron transfer was chemically irreversible. At a scan rate of 20 mV/s, there was a cathodic peak at −0.56 V vs SCE, corresponding to the redox pair Pd(II)/Pd(I). There were no anodic peaks observed on the reverse scan or peaks indicative of oxidative electrochemistry upon initial scanning from 0 to +1.8 V. The latter behavior is similar to that reported by Champness et al. for $[Pd(16Se4)][PF_6]_2$ in MeCN.[5] A plot of the cathodic peak current versus the square root of the scan rate was a straight line, indicating that the electrode process was a diffusion controlled process. When the potential was swept further in the cathodic direction, a broad cathodic peak appeared at −1.06 V vs SCE, which was attributed to the redox pair Pd(I)/Pd. Similar results were obtained with a carbon electrode.

The cyclic voltammogram of **2** showed a cathodic peak corresponding to the redox pair Pd(II)/Pd(I) at −0.47 V vs SCE at a scan rate of 50 mV/s in the cathodic direction. When the potential was scanned further in the cathodic direction, a second cathodic current peak appeared at −0.75 V, which was attributed to the redox pair Pd(I)/Pd. There was a broad peak at −0.41 V on the reverse scan, the position of which was not dependent on the scan rates (the cathodic current peak at −0.47 V moved to the more cathodic direction as the scan rates increased). Therefore, the peak at −0.41 V was probably caused by a species adsorbed on the electrode surface. As for **1**, an initial scan from 0 to +1.8 V showed no anodic peaks indicative of oxidative electrochemistry.

Crystal Structures. Rigid-body thermal motion analysis[16] for the cation of **1** yielded $R_w = 0.048$ for the agreement between observed and calculated *U(ij)* with slight excess motion for some carbon atoms. A more detailed analysis[17] of the carbon atom motions was deemed unwarranted because of the errors. An apparently short bond length (C(1)−C(2), 1.45(1) Å) is unlikely to be genuine and may merely be an artifact of unmodeled internal motion. However, it could also be a consequence of unresolved disorder or perhaps of lower symmetry since C(1) lies on a crystallographic mirror plane. Nevertheless, the development of more complex models involving lower symmetry or disorder was rejected, because of the good structure factor agreement ($R = 0.036$) and the physically reasonable thermal motion (albeit large). The overall thermal motion for the more precisely determined structure, **2**, is significantly lower than that for **1**. The motion of the cation was modeled very well by a rigid body analysis ($R_w = 0.038$ for observed and calculated *U(ij)*) with no significant excess motion. Only the corrections to the Pd−Se bond lengths were significant in terms of the least-squares errors. The corrected values for the Pd−Se bond lengths are included in Tables 2 and 3 along with the uncorrected bond lengths, bond angles, and torsion angles for the cations of **1** and **2**, respectively.

Both **1** and **2** contain the complex cation $[Pd(16Se4)]^{2+}$ in which Pd is centrally bound by the four Se atoms in a square-planar arrangement (Figures 1 and 2). In either case the configuration of the complex cation can be described as *c*,*c*,*c*[10] (i.e., the nonbonding electron pairs of all four Se atoms are directed toward one side of the coordination plane). In the case of **1** a crystallographic mirror plane bisects the molecule, passing through atoms Pd, C(1), and C(9). In both **1** and **2**, however, the cation has approximate *mm* (C_{2v}) symmetry. The molecular conformation (characterized by the bond torsion angles given in Tables 2 and 3) can be described as having alternate chair and boat forms of the fused six-membered metallocycles about Pd. This results in an edge-to-edge compression of the "square-planar" complex with the more acute Se−Pd−Se bond angles belonging to the chair-formed rings.

The Pd−Se bond distances (see Tables 2 and 3) are comparable with previous values (*cf.* Pd−Se, 2.429(1)[18] and 2.424(7)[19] Å in Pd(II) complexes of dialkylseleno ethers and 2.428(1) and 2.435(2) Å in $[Pd(16Se4)][PF_6]_2 \cdot 2MeCN$ [5]). The relatively high precision in the structure of **2** clearly reveals a small but significant asymmetry in the Pd−Se bond lengths to *trans*-related selenium atoms. This is matched and possibly explained by a trapezoidal distortion of the plane figure defined by the four selenium atoms (*cf.* the unequal opposing bond angles Se(3)−Pd−Se(7), 84.89(2)°, and Se(11)−Pd−Se(15), 81.12(2)°). It is not possible to say whether this asymmetry derives from packing effects and the low crystallographic symmetry or whether it represents a minimum energy state of the free complex; however, such asymmetry in chemically equivalent bonds is noteworthy. An analogous distortion in the

Table 2. Selected Bond Distances (Å), Angles (deg), and Torsion Angles (deg) for $[Pd(16Se4)][BF_4]_2$ (**1**)

Distances			
Pd−Se(3)	2.423(1) {2.429}[a]	Pd−Se(7)	2.432(1) {2.438}
Se(3)−C(2)	1.94(1)	Se(7)−C(6)	1.96(1)
Se(3)−C(4)	1.94(1)	Se(7)−C(8)	1.945(9)
C(1)−C(2)	1.45(1)	C(5)−C(6)	1.51(2)
C(4)−C(5)	1.52(1)	C(8)−C(9)	1.51(1)

Angles			
Se(3)−Pd−Se(3)′[b]	98.67(7)	C(4)−Se(3)−Pd	99.5(3)
Se(7)−Pd−Se(3)	81.27(4)	C(4)−Se(3)−C(2)	98.6(5)
Se(7)−Pd−Se(3)′	177.90(7)	C(6)−Se(7)−Pd	100.3(4)
Se(7)−Pd−Se(7)′	98.71(7)	C(8)−Se(7)−Pd	112.3(3)
C(2)−Se(3)−Pd	112.8(3)	C(8)−Se(7)−C(6)	98.1(5)
C(1)−C(2)−Se(3)	119.2(10)	C(2)−C(1)−C(2)′	119.4(17)
C(5)−C(4)−Se(3)	111.9(8)	C(6)−C(5)−C(4)	118.4(11)
C(5)−C(6)−Se(7)	113.4(8)	C(8)−C(9)−C(8)′	112.2(14)
C(9)−C(8)−Se(7)	116.8(9)		

Torsion Angles	
C(2)′−C(1)−C(2)−Se(3)	−74.2(9)
C(4)−Se(3)−C(2)−C(1)	−78.7(8)
C(2)−Se(3)−C(4)−C(5)	−168.4(10)
Se(3)−C(4)−C(5)−C(6)	−67.8(8)
Se(7)−Pd−Se(3)−C(2)	−174.6(4)
Se(7)−Pd−Se(3)−C(4)	−71.0(3)
Se(3)′−Pd−Se(3)−C(2)	7.6(3)
Se(3)′−Pd−Se(3)−C(4)	111.1(3)
Se(3)−Pd−Se(7)−C(6)	68.9(4)
Se(3)−Pd−Se(7)−C(8)	172.1(3)
C(4)−C(5)−C(6)−Se(7)	65.5(8)
C(8)−Se(7)−C(6)−C(5)	173.2(10)
C(6)−Se(7)−C(8)−C(9)	76.1(7)
Se(7)−C(8)−C(9)−C(8)′	82.0(8)
Se(7)′−Pd−Se(7)−C(6)	−113.3(4)
Se(7)′−Pd−Se(7)−C(8)	−10.0(3)
Pd−Se(3)−C(2)−C(1)	25.5(6)
Pd−Se(3)−C(4)−C(5)	76.6(7)
Pd−Se(7)−C(6)−C(5)	−72.2(7)
Pd−Se(7)−C(8)−C(9)	−28.6(5)

[a] The values in { } include a correction for rigid-body thermal motion of the non-hydrogen atoms of the complex cation. [b] Prime denotes = *x*, $^1/_2 - y$, *z*.

(16) Shomaker, V.; Trueblood, K. N. *Acta Crystallogr., Sect. B* **1968**, *24*, 63.
(17) Maverick, E.; Seiler, P.; Schweizer, W. B.; Dunitz, J. D. *Acta Crystallogr., Sect. B* **1980**, *36*, 615.
(18) Chadha, R. K.; Chehayber, J. M.; Drake, J. E. *Inorg. Chem.* **1986**, *25*, 611.
(19) Skakke, P. E.; Rasmussen, S. E. *Acta Chem. Scand.* **1970**, *24*, 2634.

Table 3. Selected Bond Distances (Å), Angles (deg), and Torsion Angles (deg) for [Pd(16Se4)][BF_4]Cl (**2**)

Distances

Pd−Se(3)	2.4560(7) {2.460}[a]	Pd−Se(11)	2.4395(7) {2.444}
Pd−Se(7)	2.4583(7) {2.463}	Pd−Se(15)	2.4430(7) {2.447}
Se(3)−C(2)	1.973(6)	Se(11)−C(10)	1.944(6)
Se(3)−C(4)	1.959(5)	Se(11)−C(12)	1.962(5)
Se(7)−C(6)	1.958(6)	Se(15)−C(14)	1.965(5)
Se(7)−C(8)	1.965(5)	Se(15)−C(16)	1.944(6)
C(1)−C(2)	1.500(8)	C(8)−C(9)	1.487(8)
C(1)−C(16)	1.516(8)	C(9)−C(10)	1.502(8)
C(4)−C(5)	1.523(7)	C(12)−C(13)	1.504(8)
C(5)−C(6)	1.517(8)	C(13)−C(14)	1.510(8)

Angles

Se(7)−Pd−Se(3)	84.89(2)	Se(15)−Pd−Se(3)	96.14(2)
Se(11)−Pd−Se(3)	170.03(3)	Se(15)−Pd−Se(7)	166.97(2)
Se(11)−Pd−Se(7)	95.63(2)	Se(15)−Pd−Se(11)	81.12(2)
C(2)−Se(3)−Pd	111.6(2)	C(10)−Se(11)−Pd	112.2(2)
C(4)−Se(3)−Pd	102.4(2)	C(12)−Se(11)−Pd	102.2(2)
C(4)−Se(3)−C(2)	94.5(3)	C(12)−Se(11)−C(10)	94.6(3)
C(6)−Se(7)−Pd	102.0(2)	C(14)−Se(15)−Pd	100.5(2)
C(8)−Se(7)−Pd	110.9(2)	C(16)−Se(15)−Pd	110.8(2)
C(8)−Se(7)−C(6)	95.1(3)	C(16)−Se(15)−C(14)	96.1(3)
C(16)−C(1)−C(2)	113.8(5)	C(10)−C(9)−C(8)	115.2(5)
C(1)−C(2)−Se(3)	116.2(4)	C(9)−C(10)−Se(11)	116.5(4)
C(5)−C(4)−Se(3)	112.4(4)	C(13)−C(12)−Se(11)	114.5(4)
C(6)−C(5)−C(4)	114.0(5)	C(14)−C(13)−C(12)	115.3(5)
C(5)−C(6)−Se(7)	113.5(4)	C(13)−C(14)−Se(15)	112.1(4)
C(9)−C(8)−Se(7)	117.7(4)	C(1)−C(16)−Se(15)	114.7(4)

Torsion Angles

C(16)−C(1)−C(2)−Se(3)	−72.6(5)
C(2)−Se(3)−C(4)−C(5)	−172.5(5)
C(4)−C(5)−C(6)−Se(7)	75.0(4)
C(6)−Se(7)−C(8)−C(9)	92.5(5)
C(8)−C(9)−C(10)−Se(11)	−78.9(5)
C(10)−Se(11)−C(12)−C(13)	−173.3(6)
C(12)−C(13)−C(14)−Se(15)	−70.6(5)
C(14)−Se(15)−C(16)−C(1)	75.6(4)
Se(7)−Pd−Se(3)−C(2)	−162.3(2)
Se(15)−Pd−Se(3)−C(2)	30.8(2)
Se(3)−Pd−Se(7)−C(6)	61.7(2)
Se(11)−Pd−Se(7)−C(6)	−128.3(2)
Se(7)−Pd−Se(11)−C(10)	26.5(2)
Se(15)−Pd−Se(11)−C(10)	−166.3(2)
Se(3)−Pd−Se(15)−C(14)	−121.3(2)
Se(11)−Pd−Se(15)−C(14)	68.3(2)
Pd−Se(3)−C(2)−C(1)	5.0(3)
Pd−Se(3)−C(4)−C(5)	74.2(3)
Pd−Se(7)−C(6)−C(5)	−73.9(4)
Pd−Se(7)−C(8)−C(9)	−12.5(3)
C(4)−Se(3)−C(2)−C(1)	−100.3(5)
Se(3)−C(4)−C(5)−C(6)	−74.7(4)
C(8)−Se(7)−C(6)−C(5)	173.4(5)
Se(7)−C(8)−C(9)−C(10)	76.4(5)
C(12)−Se(11)−C(10)−C(9)	−88.9(5)
Se(11)−C(12)−C(13)−C(14)	−67.7(5)
C(16)−Se(15)−C(14)−C(13)	169.0(6)
C(2)−C(1)−C(16)−Se(15)	88.3(5)
Se(7)−Pd−Se(3)−C(4)	−62.3(2)
Se(15)−Pd−Se(3)−C(4)	130.7(2)
Se(3)−Pd−Se(7)−C(8)	162.0(2)
Se(11)−Pd−Se(7)−C(8)	−28.0(2)
Se(7)−Pd−Se(11)−C(12)	126.7(2)
Se(15)−Pd−Se(11)−C(12)	−66.1(2)
Se(3)−Pd−Se(15)−C(16)	−20.6(2)
Se(11)−Pd−Se(15)−C(16)	169.1(2)
Pd−Se(11)−C(10)−C(9)	16.3(3)
Pd−Se(11)−C(12)−C(13)	72.8(4)
Pd−Se(15)−C(14)−C(13)	−78.4(4)
Pd−Se(15)−C(16)−C(1)	−28.1(3)

[a] The values in { } include a correction for rigid-body thermal motion for the non-hydrogen atoms of the complex cation.

case of **1**, if ordered, would violate the crystallographic mirror symmetry—a possibility we have already noted above.

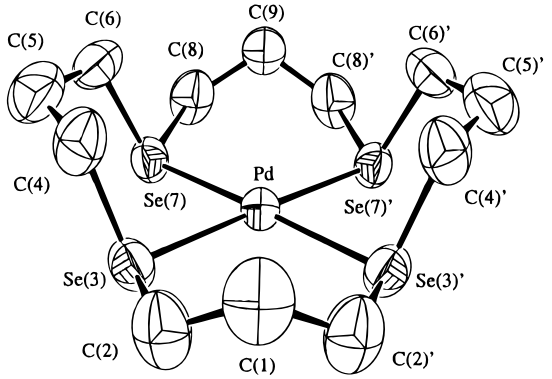

Figure 1. Structure of the $[Pd(16Se4)]^{2+}$ ion in **1**. Hydrogen atoms excluded; 50% probability displacement ellipsoids shown.

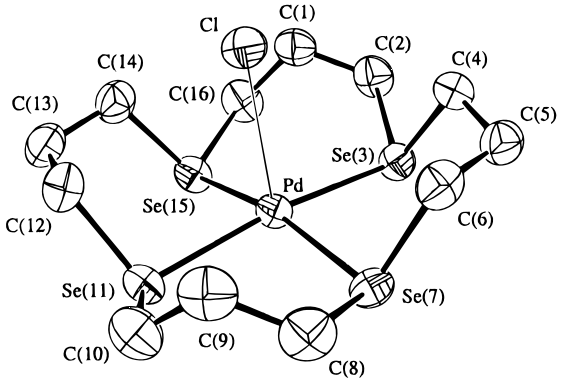

Figure 2. Structure of the $[Pd(16Se4)]^{2+}Cl^-$ ion pair in **2**. Hydrogen atoms excluded; 50% probability displacement ellipsoids shown.

In **1**, the Pd atom deviates from the precise plane of the four Se atoms by 0.045(2) Å, while in **2** the Pd atom is 0.2422(5) Å from the best least-squares plane through the four Se atoms which themselves deviate slightly (±0.032(1) Å) from coplanarity. In **2**, the degree by which the palladium atom deviates from the Se_4 plane may be attributed to an electrostatic attraction toward the Cl^- anion (shown in Figure 2) at a distance of 3.069(1) Å from the palladium atom. This is the only interionic distance in the structure of **2** which is significantly less than its corresponding sum of accepted van der Waals radii (3.38 Å). In **1**, the closest contacts between molecular ions (2.95(3) Å, Pd--F(7) and 3.18(3) Å, Se(7)--F(9)) involve fluorine atoms of the disordered BF_4^- ion (*cf.* the respective sums of accepted van der Waals radii: 3.10 Å, Pd--F and 3.37 Å, Se--F).

In principle, 16Se4 can form diastereomeric coronand complexes of four different configurations. Based on the relative orientations, with respect to the coordination plane, of the nonbonding pairs of electrons on adjacent selenium atoms, these diastereomers can be characterized as *c,c,c*; *c,t,c*; *t,t,t*; and *c,c,t*,[10] as illustrated in Figure 3. The first report of the synthesis and crystal structure of a monomeric transition metal−coronand complex of a cyclic poly(selena ether) was of [Cu(16Se4)][SO_3CF_3]$_2$.[3] Subsequently, crystal structures of *trans*-[$RhCl_2$(16Se4)][BF_4] [4] and [M(16Se4)][PF_6]$_2$·2MeCN (M = Pd, Pt)[5] have also appeared. Each of these structures contains a pseudotetragonally coordinated metal complex in which the 16Se4 ligand is in the *c,t,c* configuration. The present work represents the first observation of 16Se4 complexes having the *c,c,c* configuration.

The *c,c,c* and *c,t,c* configurations are the most commonly observed configurations in metal complexes of the analogous thia macrocycle 16S4 and related coronands. For example, 16S4 adopts the *c,c,c* configuration in three complex cations of molybdenum.[20−22] Unlike **1** and **2**, these display chair conformations for all four of their fused six-membered metallocycles

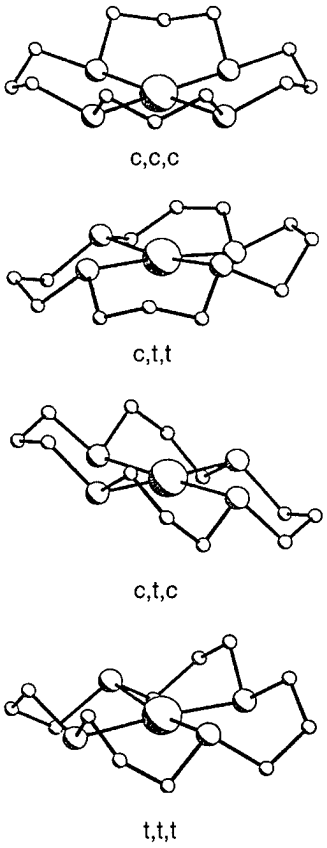

Figure 3. Four possible configurations of 16Se4 in $[Pd(16Se4)][BF_4]_2$.

and thus more closely approximate local 4mm (C_{4v}) point symmetry. The *c,t,c* configuration is observed, for $[Fe(16S4)I_2]$,[23] $[Ni(16S4)]^{2+}$,[24] $[Rh(16S4)Cl_2]$,[25] $[Cd(16S4)]^{2+}$,[26] $[Cu(16S4)]^{2+}$,[27] and $[Pd(16S4)]^{2+}$.[1b,5] Examples of *t,t,t* and *c,c,t* configurations are rare. The *t,t,t* isomer is observed in $[Hg(16S4)][ClO_4]_2$,[26,28] suggesting that larger metal ions might prefer this configuration. Molecular orbital calculations[29] of the energy required to transform 16S4 from its free conformation to some of the conformations required for square-planar complexation indicate that the conformations may be preferred in the order *c,t,c* > *c,c,c* > *t,t,t*. No calculation was made for *c,c,t*. To the best of our knowledge, the *c,c,t* configuration has not been observed in pseudotetragonal metal complexes of either 16S4 or 16Se4. However, a palladium(II) complex cation of L = 3,3,7,7,11,11,15,15-octamethyl-1,9-dithia-5,13-diazacyclohexadecane has been observed as both *c,c,c* and *c,c,t*(N) diastereomers in the same crystal structure ($[PdL]Cl_2 \cdot 2H_2O$).[10]

(20) Cragel, J., Jr.; Pett, V. B.; Glick, M. D.; DeSimone, R. E. *Inorg. Chem.* **1978**, *17*, 2885.
(21) DeSimone, R. E.; Glick, M. D. *Inorg. Chem.* **1978**, *17*, 3574.
(22) DeSimone, R. E.; Cragel, J., Jr.; Ilsley, W. H.; Glick, M. D. *J. Coord. Chem.* **1979**, *9*, 167.
(23) Hills, A.; Hughes, D. L.; Jimenez-Tenorio, M.; Leigh, G. J.; Houlton, A.; Silver, J. *J. Chem. Soc., Chem. Commun.* **1989**, 1774.
(24) Blake, A. J.; Halcrow, M. A.; Schröder, M. *J. Chem. Soc., Dalton Trans.* **1992**, 2803.
(25) Blake, A. J.; Reid, G.; Schröder, M. *J. Chem. Soc., Dalton Trans.* **1989**, 1675.
(26) Setzer, W. N.; Tang, Y.; Grant, G. J.; Van Derveer, D. G. *Inorg. Chem.* **1991**, *30*, 3652.
(27) Pett, V. B.; Diaddario, L. L., Jr.; Dockal, E. R.; Corfield, P. W.; Glick, M. D.; Ceccarelli, C.; Ochrymowycz, L. A.; Rorabacher, D. B. *Inorg. Chem.* **1983**, *22*, 3661.
(28) Jones, T. E.; Sokol, L. S. W. L.; Rorabacher, D. B.; Glick, M. D. *J. Chem. Soc., Chem. Commun.* **1979**, 140.
(29) Durrant, M. C.; Richards, R. L.; Firth, S. *J. Chem. Soc., Perkin Trans. 2* **1993**, 445.

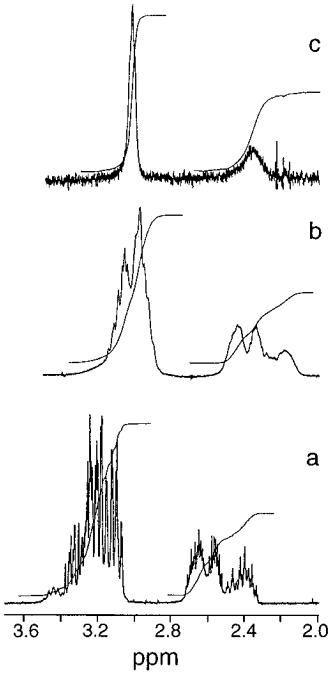

Figure 4. ^{1}H-NMR spectra of $[Pd(16Se4)]^{2+}$ recorded at (a) room temperature, (b) 354 K, (c) 389 K.

The crystal structure of $[Pd(16Se4)][PF_6]_2 \cdot 2MeCN$ contains the complex cation in the *c,t,c* configuration[5] (as does the corresponding platinum compound), whereas we observe two crystal structures (**1** and **2**) in which the same complex cation displays the *c,c,c* stereochemistry. It seems reasonable that, in the crystals of **1** and **2**, the complex cation appears in the dipolar *c,c,c* form since they contain smaller, and thus more polarizing, anions and no solvent of crystallization, whereas the centrosymmetric *c,t,c* isomer coincides with the larger PF_6^- anions and two solvent molecules of crystallization.[5] The apparent coexistence of these same two diastereomers in D_2O solutions of **1** and their interconversion at moderate temperatures can be demonstrated from the NMR results (below).

Solution NMR Studies. The ^{77}Se NMR spectrum of **1**, in D_2O at ambient temperature, showed two resonances in an approximate 2:1 ratio. The ^{13}C NMR spectrum of a D_2O solution of **1**, at ambient temperature, showed six major resonances (approximate relative intensities, ~1:1.8:1:0.9:0.5:0.5) and two of much lower intensity. As the temperature was raised (to 389 K), the resonances broadened. Upon cooling to ambient temperature, the original spectrum was restored. In the corresponding variable temperature ^{1}H-NMR spectra (Figure 4), reversible line broadening and coalescence phenomena were observed. The sets of high-field multiplets (δ 2.30−2.75, rel integrated int 1), attributed to the α-CH_2 protons, and low-field multiplets (δ 3.04−3.53, rel integrated int 2), attributed to the β-CH_2 protons, each coalesced to a single broad resonance (see Figure 4). The analysis is simplified by the fact that the α resonances in both ^{13}C and ^{1}H spectra appear downfield from the β resonances. Figure 5 shows the inverse ^{1}H−^{13}C correlated 2D NMR spectrum of **1** in D_2O at ambient temperature. The ^{13}C-NMR signal at 26.7 ppm correlated with only the ^{1}H multiplet centered at δ ~2.58, suggesting that the two protons of the corresponding β-CH_2 group are chemically equivalent. The ^{13}C signals at 29.8 and 30.0 ppm both correlated with two different ^{1}H multiplets (centered at ~2.66 and ~2.40 ppm), indicating two chemically distinct protons in each of the corresponding β-CH_2 groups.

Assuming that the $[Pd(16Se4)]^{2+}$ ion persists in D_2O solution, the only reasonable interpretation which is entirely consistent

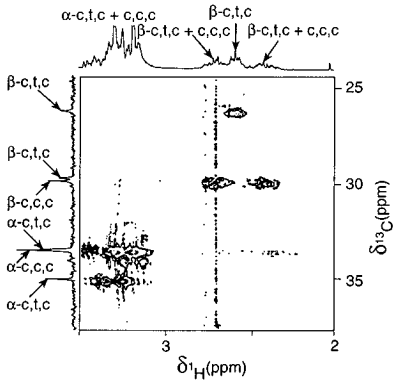

Figure 5. Inverse $^1H-^{13}C$ correlated 2D NMR spectrum of $[Pd(16Se4)]^{2+}$ recorded at ambient temperature.

Table 4. Relationship between Symmetry of the Ligand Configuration with the Number of Uncoupled NMR Absorption Lines

		no. of absorp lines (area ratio)		
config	symmetry	^{77}Se NMR	^{13}C NMR	^{1}H NMR
c,c,c	4*mm*	1	2 (2:1)	4 (2:2:1:1)
c,t,c	2/*m*	1	4 (2:2:1:1)	7 (2:2:2:2:2:1:1)
t,t,t	4*m*	1	2 (2:1)	3 (1:1:1)
c,c,t	*m*	3 (1:2:1)	6 (1:1:1:1:1:1)	12 2(1:1:1:1:1:1)

with the collected NMR results is that the major species present are the *c,t,c* and *c,c,c* isomers with the former predominating. Furthermore, it can be inferred that, at room temperature, conformational equilibration is rapid relative to the NMR time scales but that configurational exchange is slow. The coalescences observed in the variable temperature ^{1}H-NMR spectra indicate that at 389 K the rapid interconversion of the different stereoisomers is the dynamic process under observation.

Table 4 relates the highest possible point symmetry for each configuration of the square-planar complex, with the expected number and relative intensities of fully decoupled NMR absorption signals for each type of nucleus. These should conform to the results of rapid conformational exchange. On the basis of the observed number of lines in the ^{77}Se and ^{13}C NMR spectra, of **1** in D_2O at room temperature, and the observed relative intensities in the latter spectrum, the presence of the *c,c,t* isomer can be virtually ruled out. It is possible that different selenium resonances could be overlapping, but this is of low probability considering the broad range of ^{77}Se chemical shifts (2000 ppm) and their sensitivity to the chemical environment (six times larger than ^{13}C).[30] Even supposing such a coincidence did occur in the ^{77}Se spectrum, the relative intensities of the six peaks in the ^{13}C spectrum and the $^1H-^{13}C$ correlations observed in the 2D spectrum (Figure 5) imply the coexistence of more than one diastereomer. Consequently, the number of coincidences required to arrive at an interpretation which includes the *c,c,t* isomer make its presence in observable concentration highly improbable. To the best of our knowledge, the *c,c,t* configuration has never been observed in square-planar complexes of 16Se4 or 16S4. We thus discount the presence of significant concentrations of the *c,c,t* isomer of $[Pd(16Se4)]^{2+}$ in this solution. Therefore, the two observed ^{77}Se NMR absorption peaks are attributed to two different configurations of the complex since each of the remaining configurations should show only one ^{77}Se NMR signal because of their symmetry.

Since there are six major resonances observed in the ^{13}C-NMR spectrum, we assume the presence of the *c,t,c* isomer (four resonances) and either *c,c,c* or *t,t,t* (two resonances; see Table 4). These are the only consistent interpretations which do not require the assumption of coincident resonances in the ^{77}Se- and ^{13}C-NMR spectra. The additional fact that there are two β-^{13}C resonances (29.8, 30.0 ppm) which each correlate with two different ^{1}H signals indicates that the second major component is the *c,c,c* isomer. We thus arrive at an unique interpretation for the isomeric composition of the solution.

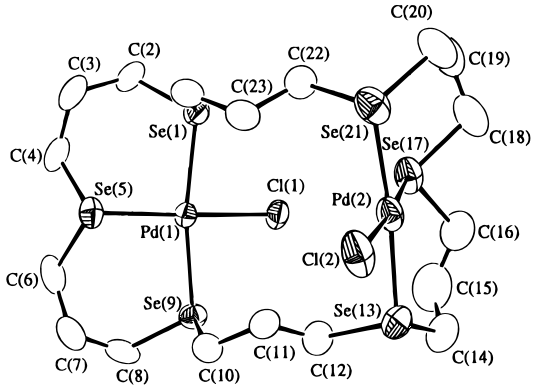

Figure 6. Molecular structure of $[(PdCl)_2(24Se6)]^{2+}$ in **3**·$2CH_2Cl_2$. Hydrogen atoms excluded; 50% probability displacement ellipsoids shown.

Our proposed assignments of the ^{13}C and ^{1}H resonances are shown on the heteronuclear two-dimensional $^1H-^{13}C\{^1H\}$ NMR spectrum (Figure 5). As indicated in Table 4, the *c,c,c* isomer should ideally show two ^{13}C peaks in a 2:1 ratio corresponding to the α and β carbon atoms, respectively. The *c,t,c* isomer would have four ^{13}C resonances (rel int 2:2:1:1) corresponding to the two chemically different α and two chemically different β carbon atoms, respectively. The highest possible point symmetry for the *c,t,c* configuration is 2/*m* (C_{2h}), where the 2-fold axis intersects two opposing β-carbon atoms and the perpendicular mirror plane intersects the complementary pair of β-carbon atoms and their associated protons. Thus, the protons on the β-CH_2 groups in the mirror plane are of two chemically distinct types, whereas those protons on the axial β-carbon atoms are all chemically equivalent. It follows that there should be three distinct β-^{1}H resonances of the *c,t,c* isomer: two of relative intensities 1:1 (δ ~2,40, 2.66 ppm), that correlate with a single ^{13}C resonance (δ 29.8 ppm) and one, of relative intensity 2 (δ ~2.58 ppm), that correlates with a second ^{13}C resonance (δ 26.3 ppm). The *c,c,c* isomer will have 4*mm* (C_{4v}) symmetry, giving an unique β-carbon resonance (δ 30.0 ppm) which correlates with two chemically distinct proton resonances of equal intensity. We deduce that the two resulting ^{1}H signals overlap with two of those of the *c,t,c* isomer, as shown in Figure 5. The assignments of the α-carbon resonances follow from the relative intensities of these peaks. The assignments are corroborated by the numbers and relative intensities of the signals in the ^{77}Se, ^{1}H, ^{13}C, and 2D $^1H-^{13}C$ NMR spectra. Thus, we conclude that there are two major isomers in solution, and they have the *c,t,c* and *c,c,c* configurations, in the approximate ratio 1.6:1. Minor cross-peaks in the $^1H-^{13}C$ correlated spectrum may be attributable to traces of other isomers. We speculate that the interconversion of the diastereomers at elevated temperatures takes place via pyramidal inversion,[31,32] although the dissociation−recombination pathway cannot be ruled out.

Pd(II) Complex of 24Se6. A 2:1 mixture of $PdCl_2$:24Se6 in MeCN yielded a yellow complex whose microanalysis was consistent with the formula $[(PdCl)_2(24Se6)][BF_4]_2$.

(30) Paulmier, C. *Selenium Reagents and Intermediates in Organic Synthesis*; Pergamon: New York, 1986; p 17.

Table 5. Selected Bond Distances (Å), Angles (deg), and Torsion Angles (deg) for $[(PdCl)_2(24Se6)][BF_4]_2 \cdot 2CH_2Cl_2$ (**3**·$2CH_2Cl_2$) at 195 K

Distances

Pd(1)−Se(1)	2.428(1)	Se(1)−C(2)	1.961(9)	Se(17)−C(16)	1.97(1)	C(10)−C(11)	1.52(1)
Pd(1)−Se(5)	2.372(1)	Se(1)−C(24)	1.963(9)	Se(17)−C(18)	1.94(1)	C(11)−C(12)	1.50(1)
Pd(1)−Se(9)	2.428(1)	Se(5)−C(4)	1.96(1)	Se(21)−C(20)	1.96(1)	C(14)−C(15)	1.51(2)
Pd(1)−Cl(1)	2.343(2)	Se(5)−C(6)	1.953(9)	Se(21)−C(22)	1.954(9)	C(15)−C(16)	1.48(2)
Pd(2)−Se(13)	2.428(1)	Se(9)−C(8)	1.934(9)	C(2)−C(3)	1.53(1)	C(18)−C(19)	1.50(2)
Pd(2)−Se(17)	2.364(1)	Se(9)−C(10)	1.954(9)	C(3)−C(4)	1.52(1)	C(19)−C(20)	1.51(1)
Pd(2)−Se(21)	2.421(1)	Se(13)−C(12)	1.961(9)	C(6)−C(7)	1.51(1)	C(22)−C(23)	1.49(1)
Pd(2)−Cl(2)	2.351(3)	Se(13)−C(14)	1.97(1)	C(7)−C(8)	1.53(1)	C(23)−C(24)	1.52(1)

Angles

Se(5)−Pd(1)−Se(1)	92.34(4)	C(6)−Se(5)−Pd(1)	106.9(3)	C(3)−C(4)−Se(5)	114.8(7)
Se(9)−Pd(1)−Se(1)	169.83(4)	C(6)−Se(5)−C(4)	94.1(4)	C(7)−C(6)−Se(5)	112.6(6)
Se(9)−Pd(1)−Se(5)	96.62(4)	C(8)−Se(9)−Pd(1)	113.1(3)	C(8)−C(7)−C(6)	113.0(8)
Cl(1)−Pd(1)−Se(1)	85.61(7)	C(10)−Se(9)−Pd(1)	103.6(3)	C(7)−C(8)−Se(9)	118.1(7)
Cl(1)−Pd(1)−Se(5)	174.68(7)	C(10)−Se(9)−C(8)	96.3(4)	C(11)−C(10)−Se(9)	113.4(6)
Cl(1)−Pd(1)−Se(9)	85.05(7)	C(12)−Se(13)−Pd(2)	104.5(3)	C(12)−C(11)−C(10)	113.2(8)
Se(17)−Pd(2)−Se(13)	97.77(5)	C(14)−Se(13)−Pd(2)	113.9(4)	C(11)−C(12)−Se(13)	112.9(7)
Se(21)−Pd(2)−Se(13)	170.71(5)	C(14)−Se(13)−C(12)	97.7(5)	C(15)−C(14)−Se(13)	115.2(8)
Se(21)−Pd(2)−Se(17)	90.77(5)	C(16)−Se(17)−Pd(2)	108.0(4)	C(16)−C(15)−C(14)	115.7(13)
Cl(2)−Pd(2)−Se(13)	84.63(9)	C(18)−Se(17)−Pd(2)	104.0(3)	C(15)−C(16)−Se(17)	115.0(8)
Cl(2)−Pd(2)−Se(17)	174.37(8)	C(18)−Se(17)−C(16)	95.5(5)	C(19)−C(18)−Se(17)	112.3(8)
Cl(2)−Pd(2)−Se(21)	86.54(9)	C(20)−Se(21)−Pd(2)	110.8(4)	C(20)−C(19)−C(18)	115.1(10)
C(2)−Se(1)−Pd(1)	110.1(3)	C(22)−Se(21)−Pd(2)	103.0(3)	C(19)−C(20)−Se(21)	118.7(8)
C(24)−Se(1)−Pd(1)	102.6(3)	C(22)−Se(21)−C(20)	99.9(5)	C(23)−C(22)−Se(21)	110.2(6)
C(24)−Se(1)−C(2)	99.6(4)	C(3)−C(2)−Se(1)	117.0(6)	C(24)−C(23)−C(22)	114.9(8)
C(4)−Se(5)−Pd(1)	104.6(3)	C(4)−C(3)−C(2)	114.7(8)	C(23)−C(24)−Se(1)	110.1(6)

Torsion Angles

C(24)−Se(1)−C(2)−C(3)	−53.9(6)	Se(17)−C(18)−C(19)−C(20)	79.6(8)	Se(13)−Pd(2)−Se(17)−C(16)	−29.6(4)
C(2)−Se(1)−C(24)−C(23)	−175.8(8)	C(18)−C(19)−C(20)−Se(21)	−62.4(7)	Se(13)−Pd(2)−Se(17)−C(18)	−130.3(3)
C(6)−Se(5)− C(4)−C(3)	178.3(8)	Se(21)−C(22)−C(23)−C(24)	170.7(10)	Se(21)−Pd(2)−Se(17)−C(16)	154.0(4)
C(4)−Se(5)−C(6)−C(7)	175.5(8)	C(22)−C(23)−C(24)−Se(1)	66.2(6)	Se(21)−Pd(2)−Se(17)−C(18)	53.4(3)
C(10)−Se(9)−C(8)−C(7)	67.4(6)	Se(5)−Pd(1)−Se(1)−C(2)	−44.4(3)	Se(17)−Pd(2)−Se(21)−C(20)	−42.8(3)
C(8)−Se(9)− C(10)−C(11)	−175.0(8)	Se(5)−Pd(1)−Se(1)−C(24)	60.9(3)	Se(17)−Pd(2)−Se(21)−C(22)	63.2(3)
C(14)−Se(13)−C(12)−C(11)	−170.0(8)	Cl(1)−Pd(1)−Se(1)−C(2)	140.5(3)	Cl(2)−Pd(2)−Se(21)−C(20)	142.1(3)
C(12)−Se(13)−C(14)−C(15)	70.2(8)	Cl(1)−Pd(1)−Se(1)−C(24)	−114.2(3)	Cl(2)−Pd(2)−Se(21)−C(22)	−111.8(3)
C(18)− Se(17)−C(16)−C(15)	168.3(11)	Se(1)−Pd(1)−Se(5)−C(4)	50.1(3)	Pd(1)−Se(1)−C(2)− C(3)	53.5(5)
C(16)−Se(17)−C(18)−C(19)	171.1(9)	Se(1)−Pd(1)−Se(5)−C(6)	149.0(3)	Pd(1)−Se(1)−C(24)−C(23)	70.9(5)
C(22)− Se(21)−C(20)−C(19)	−59.9(7)	Se(9)−Pd(1)−Se(5)−C(4)	−134.8(3)	Pd(1)−Se(5)−C(4)−C(3)	−73.1(6)
C(20)−Se(21)−C(22)−C(23)	−174.4(8)	Se(9)−Pd(1)−Se(5)−C(6)	−35.8(3)	Pd(1)−Se(5)−C(6)−C(7)	68.9(5)
Se(1)−C(2)− C(3)−C(4)	−66.4(6)	Se(5)−Pd(1)−Se(9)−C(8)	25.7(3)	Pd(1)−Se(9)−C(8)−C(7)	−40.3(5)
C(2)−C(3)− C(4)−Se(5)	78.5(7)	Se(5)−Pd(1)−Se(9)−C(10)	−77.3(3)	Pd(1)−Se(9)−C(10)−C(11)	−59.4(5)
Se(5)−C(6)− C(7)−C(8)	−87.2(8)	Cl(1)−Pd(1)−Se(9)−C(8)	−159.4(3)	Pd(2)−Se(13)−C(12)−C(11)	−52.8(5)
C(6)−C(7)− C(8)−Se(9)	69.8(7)	Cl(1)−Pd(1)−Se(9)−C(10)	97.6(3)	Pd(2)−Se(13)−C(14)−C(15)	−39.5(6)
Se(9)−C(10)−C(11)−C(12)	−61.6(6)	Se(17)−Pd(2)−Se(13)−C(12)	−82.7(3)	Pd(2)−Se(17)−C(16)−C(15)	61.6(7)
C(10)−C(11)−C(12)−Se(13)	−167.7(10)	Se(17)−Pd(2)−Se(13)−C(14)	22.8(4)	Pd(2)−Se(17)−C(18)−C(19)	−78.7(6)
Se(13)−C(14)−C(15)−C(16)	71.6(9)	Cl(2)−Pd(2)−Se(13)−C(12)	92.2(3)	Pd(2)− Se(21)−C(20) C(19)	48.2(6)
C(14)−C(15)−C(16)−Se(17)	−86.7(10)	Cl(2)−Pd(2)− Se(13)−C(14)	−162.3(4)	Pd(2)− Se(21)−C(22)−C(23)	71.4(5)

Electrochemistry. A cyclic voltammogram of $[(PdCl)_2(24Se6)][BF_4]_2$ (**3**) was recorded using a carbon electrode in MeCN (0.1 M Et_4NClO_4)). Identical results were obtained with a Pt electrode. The electron transfer was irreversible. At a scan rate of 50 mV/s, the cathodic potential peak that corresponds to the redox pair Pd(II)/Pd(I) appeared at −0.58 V vs SCE. That reduction was a one-electron transfer process for each Pd(II) ion was confirmed by a Coulometric study (see below). When the potential was scanned further in the cathodic direction, a second cathodic potential peak at −1.02 V was observed, which corresponds to the redox pair Pd(I)/Pd, as indicated by the deposition of black Pd metal on the Pt electrode surface. There were no anodic peaks observed on the reverse scan. A straight line was obtained from a plot of the cathodic peak currents vs the square root of the scan rates, indicating that the electrode process is diffusion controlled.

Electrolysis of $[(PdCl)_2(24Se6)][BF_4]_2$ (**3**) on Pt electrodes was performed at an applied potential of −0.8 V vs SCE. The yellow solution turned orange. The total electric charge passed through the solution corresponded to a two-electron process. Because **3** contains two Pd(II) ions, we conclude that each Pd ion accepted one electron from the electrode. The irreversible reduction of the complex **3** may be attributed to the coupling reaction of Pd(I) complexes, forming Pd(I)/Pd(I) metal−metal bonded dimers.[1]

Crystal Structure. In the structure of **3**·$2CH_2Cl_2$, 24Se6 chelates two individual palladium atoms in a tridentate fashion, while a chlorine atom occupies the fourth coordination site in each case, to form the $[(PdCl)_2(24Se6)]^{2+}$ cation shown in Figure 6. Selected bond distances and angles are listed in Table 5. The Pd−Se bond distances are in the expected range (see above), as are Pd−Cl, and display variations as expected for the differing trans influences of Cl and Se.

Both Pd environments are approximately square planar but show significant pyramidal distortion. The two square planes have a relative dihedral angle of approximately 48° and the chlorine atoms protrude from opposite sides of the 24Se6 ring, similarly to those in the complex cation $[Pd_2Cl_2(18N2S4)]^{2+}$ [33] (where 18N2S2 = 1,4,10,13-tetrathia-7,16-diazacyclooctadecane). There are no intramolecular interactions between the

(31) Abel, E. W.; Bhargava, S. K.; Orrell, K. G. In *Progress in Inorganic Chemistry*; Lippard, S. J., Ed.; Wiley: New York, 1984; Vol. 32, pp 1−118.
(32) Orrell, K. G. *Coord. Chem. Rev.* **1989**, *96*, 1.

palladium atoms or between a palladium atom and the chlorine atom bound to the other palladium atom.

The closest intermolecular interactions are mutual Pd(1)-Cl(1) distances of 3.258(3) Å between molecules related to one another by the inversion center at ($^1/_2$,0,0). A similar relationship exists for Pd(2)--Cl(2), 3.188(3) Å, about the inversion center at (0,0,0) (sum of accepted van der Waals radii = 3.38 Å for Pd and Cl). These interactions are consistent with the pyramidal distortions at Pd; *i.e.*, the palladium atoms are slightly drawn out of the primary coordination planes, as defined by the two sets of three selenium atoms, in the directions of the chlorine atoms of the adjacent molecules (Pd(1), 0.094(1) Å; Pd(2), 0.071(2) Å), while the respective chlorine atoms within the molecule are displaced slightly in the opposite sense with respect to the same planes (Cl(1), 0.017(3) Å; Cl(2), 0.063(4) Å). The associated intermolecular Pd--Pd distances are 3.795-(2) Å for Pd(1) and 3.983(2) Å for Pd(2) which distances do not represent significant interactions.

There are, potentially, 15 different diastereomers of $[(PdCl)_2(24Se6)]^{2+}$, only one of which is found in the crystal structure—that which displays a *trans* relationship for the orientations of every pair of adjacent pyramidal selenium centers proceeding about the ring. The four six-membered metallocycles are all in approximate chair conformations. While the highest possible point symmetry for this particular configuration is 2/*m* (C_{2h}), the observed molecule has no crystallographic point symmetry and adopts a conformation which only roughly approximates *m* (C_s) molecular point symmetry, where the Pd, Cl, Se(5), and Se(17) atoms lie approximately in the local mirror plane. This approximate symmetry is exemplified by the sequence of C−Se−C−C and Se−C−C−C bond torsion angles around the 24Se6 ring which define its conformation. Qualitatively, this sequence can be described as $AG^-G^+G^+AG^-AAG^+G^+G^-AAG^+G^-G^-AAG^+AG^-G^-G^+A$ (where *A* represents *anti* and G^+ and G^- represent positive and negative *gauche* relationships) starting with the C(4)−Se(5)−C(6)−C(7) segment (*anti*) and proceeding counterclockwise around the ring, as shown in Figure 6. Clearly, this conformation for the 24Se6 ring bears little resemblance to that previously found for the uncomplexed ligand,[2] in which four of the six selenium atoms were exodentate. Nevertheless, the buckled-quadrangular structure shown by the latter does suggest a predilection toward two coordination sites.

While the solution structure of $[(PdCl)_2(24Se6)]^{2+}$ will be the subject of further studies, it is reasonable to speculate that, like the 16Se4 complexes, both conformational and configurational interconversions will occur in solution. It is further expected that this species will display very interesting chemistry as a consequence of the binuclear nature and the possibilities for direct or ligand mediated metal−metal interactions.

Summary

The complex cation $[Pd(16Se4)]^{2+}$ which previously [5] had only been definitively observed as the *c,t,c* diastereomer has now been found also to occur as its *c,c,c* diastereomer in crystals of its tetrafluoroborate and chloro, tetrafluoroborate salts. Furthermore, multinuclear, variable temperature, and two-dimensional NMR spectroscopic results have demonstrated that aqueous solutions of $[Pd(16Se4)][BF_4]_2$, at room temperature, contain the *c,t,c* and *c,c,c* forms as the predominant species. At elevated temperatures, ^{1}H NMR spectroscopy reveals that configurational interconversion is taking place. The observed *c,t,c*:*c,c,c* ratio of ∼1.6 at room temperature is an equilibrium composition in these solutions. The complete assignment of the corresponding ^{77}Se-, ^{13}C-, and ^{1}H-NMR signals has been achieved.

Extension of this work to the 24Se6 macrocycle has produced the complex cation $[(PdCl)_2(24Se6)]^{2+}$. The crystal structure of a tetrafluoroborate salt−solvate of this cation presents one of fifteen possible diastereomers of an interesting binuclear complex.

Acknowledgment. We are grateful to the Natural Sciences and Engineering Research Council of Canada for financial support.

Supporting Information Available: Text giving additional crystallographic details and tables listing atomic parameters, anisotropic displacement parameters, distances, and angles (10 pages). See any current masthead page for ordering information.

IC951151J

(33) Blake, A. J.; Reid, G.; Schröder, M. *J. Chem. Soc., Dalton Trans.* **1990**, 3363.